

## Distribution of thermal energy during disruptions on MAST

G.F. Counsell<sup>1</sup>, F. Lott<sup>2</sup> and the MAST team,

1. EURATOM/UKAEA Fusion Association, Culham Science Centre, Abingdon, OXON OX14 3DB, UK

2. Plasma Physics Group, Blackett Laboratory, Imperial College London, SW7 2BW, UK

The spatial distribution and temporal behaviour of thermal and magnetic energy released from the core plasma during disruptions is a key area of study for ITER, as the resultant power loadings on plasma facing materials will have important implications for the allowable material choices and operational regimes. A series of experiments were conducted on MAST, as part of research co-ordinated by the EU Plasma-Wall Interaction Task Force, to explore the relationship between the disruption trigger, core thermal and magnetic energy loss, divertor target heat flux width and target heat load. Preliminary results demonstrate that the disruption heat loads are more complex than previously thought, both spatially and temporally, which may explain the scatter in data (for example in reports of target heat flux width broadening) observed between different tokamaks. The MAST data clearly shows that in at least one type of disruption, all the plasma thermal energy can be lost from the core without any broadening of the heat flux width.

Three types of disruption were studied, each terminating similar 800 kA, L-mode discharges; 1) density limit disruptions, which were reliably triggered by strong gas puffing to a Greenwald fraction of 1.2-1.3, 2) vertical displacement events (VDEs), triggered by deliberate termination of the plasma position vertical feedback and 3) disruptions triggered by the growth of a locked mode in low density, high  $\beta_{\text{pol}}$  discharges. For each case the evolution of plasma thermal energy,  $W_{\text{th}}$  and divertor target heat flux profile at all four divertor targets were determined with sub-millisecond resolution.

Due to the geometry of the spherical tokamak,  $W_{\text{th}}$  cannot be simply determined in MAST directly from the diamagnetic loop signal, which can only be used as a constraint on the plasma equilibrium solution provided by the EFIT code. EFIT, however, does not always provide reliable solutions close to disruptions and an alternative method for deriving  $W_{\text{th}}$  was employed. Measurements of the core electron temperature and density profiles were obtained during the disruption period using the MAST Thomson scattering systems, which include a multi-pulse Nd-YAG system.  $W_{\text{th}}$  was evaluated by integrating over the profiles, assuming equal ion and electron temperatures. The multi-pulse system was configured in a 'burst' mode, providing 4 pulses at up to 5 kHz, repeated every 20 ms. The evolution of  $W_{\text{th}}$  relative to the time of the disruption ( $t_{\text{dis}}$ , taken to be the peak in plasma

current at the beginning of the current redistribution) was constructed using a combination of Thomson scattering data from individual discharges and from a series of nominally identical discharges of each disruption type (i.e. where the disruption occurred at similar  $W_{th}$ ,  $I_p$ ,  $n_e$ ,  $\beta_{pol}$  etc.). The divertor target heat flux profile evolution was determined using temperature data from a fast IR camera interpreted using the THEODOR inverse heat transfer code [1]. The camera was operated at a frame rate of 1.6 kHz, which allowed a significant region of the divertor to be viewed (framing rates up to 10 kHz are possible but only with a narrow view). Measurements were obtained at each of the four divertor target regions (MAST typically operates in a double-null configuration) by moving the camera in between the repeat discharges.

In both the density limit and VDE disruptions, the thermal quench phase (characterised by a fall in  $W_{th}$  at constant  $I_p$ ) begins less than 1 ms before the current redistribution,  $0 < (t_{dis}-t) < 1$  ms. In the locked mode disruptions  $W_{th}$  falls much more gradually, beginning around 5 ms earlier at around the time a significant signal is observed on the locked

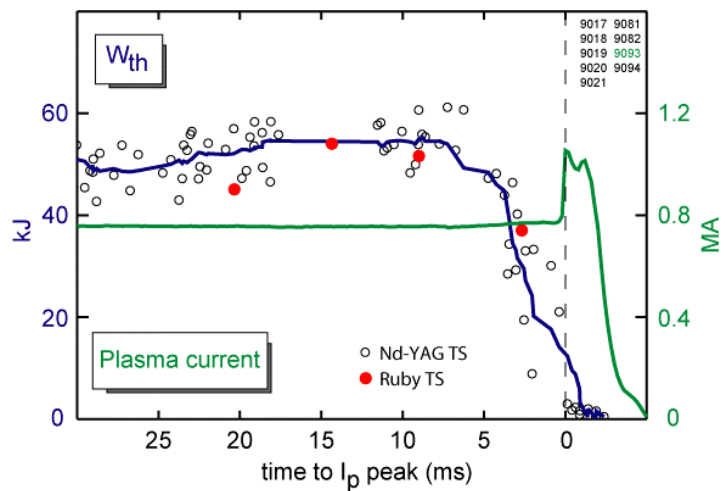


**Figure 1** Time evolution of plasma thermal energy around the time of a locked mode disruption

mode detector  $0 < (t_{dis}-t) < 6$  ms (figure 1). Unfortunately, data from the IR camera is partially saturated for the density limit and VDE disruptions in these experiments due to higher than expected heat loads and reliable target heat flux data could not be derived (this deficiency will be addressed in future work). Good quality IR data was, however, available for the locked mode shots.

The 2D surface temperature profiles show a complex, evolving structure during locked mode disruptions. Some phases of the disruption show significant production of dust, which is clearly observed on the camera and which is expelled from the divertor targets at velocities of several hundred m/s. Other phases show the formation of localised ‘hot-spots’, possibly as a result of unipolar arc formation. Significant temperature rises during the disruption are only observed in the low field side divertor and the disruption energy is apparently randomly directed to either the upper or lower target.

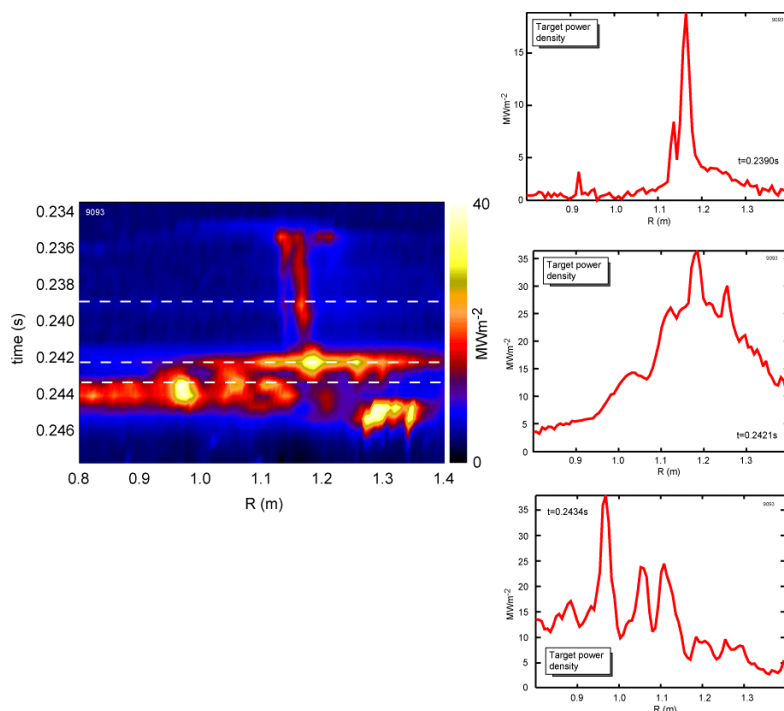


**Figure 2** False colour image of target heat flux profile during disruption, together with profiles during the thermal quench, current redistribution and current quench phases.

across the separatrix has been noted on several devices including MAST [2]). At around the time of the current redistribution,  $t \sim t_{\text{dis}}$ , the peak heat flux rises to  $\sim 40 \text{ MWm}^{-2}$  but would be much higher if it were not for a factor  $\sim 8$  increase in the heat flux width at this time. Later, at  $(t_{\text{dis}} - t) \sim 1\text{-}2$  ms during the plasma current decay, the peak heat flux remains at  $\sim 40 \text{ MWm}^{-2}$  but the heat flux becomes highly localised into multiple ‘hot-spots’. Fine surface ‘tracks’ observed on tiles removed from MAST during a recent divertor upgrade appear to provide support for the conclusion that these localised hot-spots are a result of arcing.

By spatially integrating the target heat flux profile in each IR camera frame and assuming toroidally symmetric power loads, the cumulative energy arriving to the target as a function of  $t_{\text{dis}} - t$  was determined,  $W_{\text{div}}$ . During the thermal quench,  $0 < (t_{\text{dis}} - t) < 6$  ms,  $W_{\text{div}}$  rises from 0 to  $\sim 60$  kJ, in good agreement with the decay of  $W_{\text{th}}$  over the same period. This appears to confirm that most or all of the energy arrives at a single, low field side target and indicates that THEODOR analysis of the IR camera data is probably unaffected by the ‘surface layer effects’ which hamper interpretation of other, more rapid transient heat loads (e.g. ELMs.) [3]. In the current redistribution and quench phases,  $(t_{\text{dis}} - t) < 0$  ms,  $W_{\text{div}}$  rises by a further  $\sim 200$  kJ over 1-2ms. This is close to the EFIT estimate of the  $\frac{1}{2}LI^2$  magnetic

Analysis with THEODOR in fact reveals three clear phases. During the thermal quench,  $0 < (t_{\text{dis}} - t) < 6$  ms, the target heat flux reaches  $\sim 20 \text{ MWm}^{-2}$ , compared to  $0.4 \text{ MWm}^{-2}$  for the discharge flat-top. The heat flux width, however, remains roughly unchanged from the pre-disruption period and there may even be some indication of narrowing (a weak inverse dependence of scrape-off layer width on power flow

energy of the plasma prior to the disruption of 300 kJ. The effective power loss from the core to the divertor rises to  $P_{\text{loss}} \sim 10\text{MW}$  in the thermal quench, up from  $\sim 1.3\text{MW}$  during the flat-top, and the target heat flux width is around  $\Delta_h \sim 5\text{ cm}$  (possibly unchanged within errors from the  $\sim 7\text{ cm}$  width derived using data from the target Langmuir probe arrays during the flat-top). In the current redistribution and quench,  $P_{\text{loss}}$  again rises to

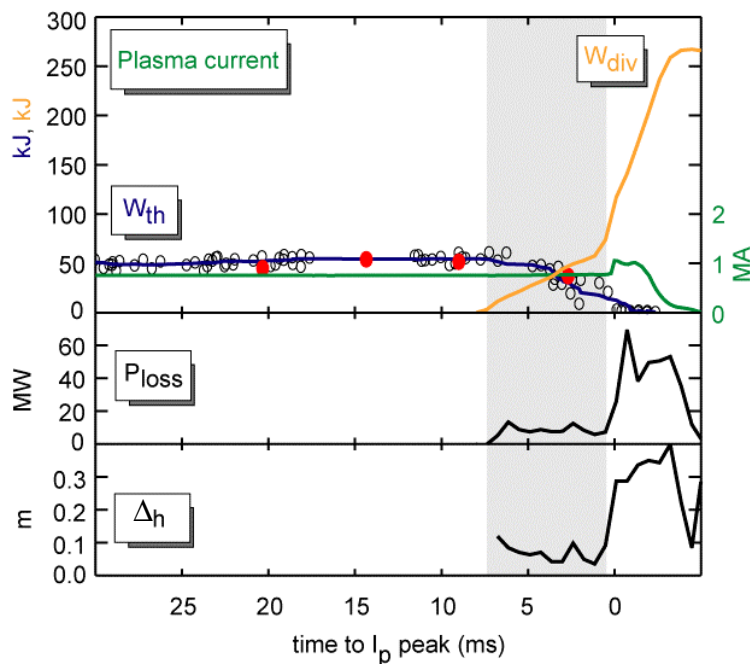


Figure 3 Time evolution of energy arriving at the target during the disruption, together with power loss from the core and target heat flux width.

$\sim 60\text{MW}$  (reflecting the loss of magnetic energy) but  $\Delta_h$  broadens by a factor 8 to around  $40\text{ cm}$ , which dramatically ameliorates the peak heat flux.

In summary, Thomson scattering in MAST can provide a good measure of  $W_{\text{th}}$  during disruptions. A preliminary investigation of disruptions arising from growth of a locked mode shows that plasma thermal energy decays over several milliseconds before the current redistribution. IR analysis of heat loads to the divertor targets in these disruptions shows that probably all of the thermal energy can be accounted for at one, low field side target. The target heat flux width remains constant or narrows in the thermal quench, resulting in a large peak heat flux. During the later current redistribution and quench phases of the disruption, however, the heat flux width broadens significantly, ameliorating the very high peak heat fluxes which would otherwise arise. If confirmed in future studies, these results are significant for ITER since target heat flux width broadening may not be relied upon to ameliorate peak heat fluxes throughout the whole period of the disruption.

This work was funded jointly by the United Kingdom Engineering and Physical Sciences Research Council and by EURATOM.

- [1] A. Herrmann *et al.*, Plasma Phys. Control. Fusion **37** (1995) 17
- [2] J-W. Ahn *et al.*, 'L-mode SOL width scaling in the MAST spherical tokamak and extrapolations to the future machine', to be submitted to Plasma Phys. Contr. Fusion (2004)
- [3] P. Andrew *et al.*, J. Nucl. Mater. **313-316** (2003) 135